

Probing the nature of the X-ray source IGR J16327-4940 with *Chandra*

L. Sidoli,^{1*} V. Sguera,² K. Postnov,^{3,4} P. Esposito,^{5,1} L. Oskinova,^{6,4} and I.A. Mereminskiy⁷

¹ *INAF, Istituto di Astrofisica Spaziale e Fisica Cosmica, via A. Corti 12, 20133 Milano, Italy*

² *INAF, Osservatorio di Astrofisica e Scienza dello Spazio, via P. Gobetti 101, 40129 Bologna, Italy*

³ *Sternberg Astronomical Institute, Lomonosov Moscow State University, Universitetskij pr. 13, 119234 Moscow, Russia*

⁴ *Kazan Federal University, Kremlyovskaya 18, 420008 Kazan, Russia*

⁵ *Scuola Universitaria Superiore IUSS Pavia, Piazza della Vittoria 15, 27100, Pavia, Italy*

⁶ *Institute for Physics and Astronomy, University Potsdam, 14476 Potsdam, Germany*

⁷ *Space Research Institute, Russian Academy of Sciences, Profsoyuznaya 84/32, 117997 Moscow, Russia*

Accepted 2023 September 18. Received 2023 September 15; in original form 2023 July 4

ABSTRACT

We report on the results of a *Chandra* observation of the source IGR J16327-4940, suggested to be a high mass X-ray binary hosting a luminous blue variable star (LBV). The source field was imaged by ACIS-I in 2023 to search for X-ray emission from the LBV star and eventually confirm this association. No X-ray emission is detected from the LBV star, with an upper limit on the X-ray luminosity of $L_{0.5-10\text{keV}} < 2.9^{(+1.6)}_{(-1.1)} \times 10^{32}$ erg s⁻¹ (at the LBV distance $d=12.7^{+3.2}_{-2.7}$ kpc). We detected 21 faint X-ray sources, 8 of which inside the *INTEGRAL* error circle. The brightest one is the best candidate soft X-ray counterpart of IGR J16327-4940, showing a hard power law spectrum and a flux corrected for the absorption $UF_{0.5-10\text{keV}}=2.5 \times 10^{-13}$ erg cm⁻² s⁻¹, implying a luminosity of $3.0 \times 10^{33} d_{10\text{kpc}}^2$ erg s⁻¹. No optical/near-infrared counterparts have been found. Previous X-ray observations of the source field with Swift/XRT and ART-XC did not detect any source consistent with the *INTEGRAL* position. These findings exclude the proposed LBV star as the optical association, and pinpoint the most likely soft X-ray counterpart. In this case, the source properties suggest a low mass X-ray binary, possibly a new member of the very faint X-ray transient class.

Key words: stars: neutron: massive - X-rays: binaries: individual: IGR J16327-4940, MN 44, EM* VRMF 55

1 INTRODUCTION

The discoveries performed by the *INTEGRAL* satellite, surveying the transient hard X-ray sky, have revitalized the field of High Mass X-ray Binaries (HMXBs; Kretschmar et al. 2019 for a review). New classes of HMXBs have been unveiled, like the so-called obscured sources (Walter et al. 2003) and the Supergiant Fast X-ray Transients (Sguera et al. 2005; Negueruela et al. 2006). The *INTEGRAL* catalogs (Bird et al. 2010, 2016) still include many unidentified hard X-ray sources (detected above 20 keV) whose nature is unclear and potentially very intriguing.

IGR J16327-4940 is one of these sources (IGRJ16327, hereafter for brevity). It was reported in the *INTEGRAL*/IBIS catalogs (Bird et al. 2010, 2016) as a faint, transient hard X-ray source, best detected in the energy band 20–100 keV only once during a short period of enhanced X-ray activity (duration of about 1 day) in March 2005. The source peak-flux was 2.1 mCrab or 1.6×10^{-11} erg cm⁻² s⁻¹ (20–40 keV). Its sky position is at R.A.=248.172°, dec=-49.666° (J2000), with an error radius of 5′ (90% c.l.). The source has not been detected in the mosaic significance map obtained by sum-

ming up all available *INTEGRAL* observations for a total of 4.8 Ms on-source exposure (Bird et al. 2016). The inferred 2 σ upper limit on the persistent emission is about 0.2 mCrab or 1.5×10^{-12} erg cm⁻² s⁻¹ (20–40 keV). To date, soft X-ray information (below 10 keV) on the source have never been reported in the literature.

The source was tentatively associated by (Masetti et al. 2010) with an early-type emission line star (EM* VRMF 55; R=15.5 mag), implying its identification with an HMXB. Further optical investigations revealed the presence of hydrogen and iron emission lines typical of luminous blue variables (LBVs; Gvaramadze et al. 2015), a strong brightness decline (from V~14.40 mag to V~15.70 mag in six years) and a significant variability in its spectral properties (it became hotter in 2015, compared to 2009). The star was also found to be surrounded by a circular nebula (named MN44) in *Spitzer* data (Gvaramadze et al. 2010; Gvaramadze 2019), another property typical among LBVs, produced by the interaction of the stellar ejected material with the interstellar medium. The stellar proper motion of MN44 and its distance ($d=5.2^{+2.7}_{-1.7}$ kpc, *Gaia* DR2, Bailer-Jones et al. 2018) led Gvaramadze (2018) to conclude that the star is running away from the Galactic plane, with a trajectory consistent

* E-mail: lara.sidoli@inaf.it

with being born in Westerlund 1, one of the most massive star clusters in our Galaxy.

We note that an updated distance value is now available and is reported in the *Gaia* EDR3 catalog ($d=12.7^{+3.2}_{-2.7}$ kpc, obtained from both the photometry and the parallax; [Bailer-Jones et al. 2021](#)). This new distance rejects the association with Westerlund 1. We adopt the new *Gaia* EDR3 distance in our paper.

In this paper we mainly report the results of a *Chandra* observation we proposed in order to unveil the LBV star as the counterpart of IGRJ16327, possibly detecting X-ray emission from its sky position.

2 OBSERVATION AND DATA REDUCTION

Chandra observed the source sky region on February 11, 2023 (ObsID 26517) with a net exposure time of 9957 s, using ACIS-I in very faint mode. The observation was targeted at the coordinates R.A. (J2000)=248.166417°, dec (J2000)=−49.703797° (the sky position of the LBV star) and aimed at imaging the whole *INTEGRAL* error circle.

The data were reduced with the *Chandra* Interactive Analysis of Observation (CIAO 4.14) and CALDB (4.9.8), adopting standard procedures. The tool `chandra_repro` was applied to reprocess the level 1 event lists. Images, exposure and point-spread-function (PSF) maps were produced by the `fluximage` tool in the energy range 0.5-7 keV, using the full resolution (pixel size of 0.492") and resulting in output images with 2284 by 2275 pixels.

A proper source detection was performed (Sect. 3.1). For sufficiently bright sources, we performed a spectral and a timing analysis. The spectroscopy was performed using `xspec` ([Arnaud 1996](#)) in *HEASoft* ([Nasa High Energy Astrophysics Science Archive Research Center 2014](#); v.29). The model `TBabs` was adopted to account for the low energy absorption in the X-ray spectra. The photoelectric absorption cross sections of [Verner et al. \(1996\)](#) and the interstellar abundances of [Wilms et al. \(2000\)](#) were used. We grouped the spectra adopting 1 count per bin and Cash statistics ([Cash 1979](#)). In the spectroscopy, all uncertainties are given at 90% confidence level for one interesting parameter. The uncertainty (90%) on the unabsorbed X-ray fluxes have been calculated using `cflux` in `xspec`.

For fainter sources, we have estimated their fluxes using `srcflux` tool in CIAO, with the appropriate response files, assuming an absorbed power law model with a photon index $\Gamma=2$ and an absorption column density $N_{\text{H}}=10^{22}$ cm $^{-2}$ (results in Table 1). The source-free backgrounds were evaluated locally from annular regions centered on the position of the sources, with an inner and an outer radius of one and five times source extraction radius (90% PSF radius at 2.4 keV). When the annular background regions overlap with nearby sources, they have been modified excising the contaminating nearby source region.

The timing analysis has been performed after correcting the arrival times of all events to the Solar System barycenter using `axbary`.

2.1 Swift

We note that the source sky region has never been observed before in soft X-rays, apart from a short *Swift*/XRT snapshot (~ 2.8 ks) performed in June 2012 (ObsID 00032483001), never reported in the literature to date. For completeness, we reduced this observation using `xrtpipeline` in *HEASoft* and extracted an image and its exposure map in the total band (0.3-10 keV). We did not detect any source within the XRT field-of-view (FOV). Using `sosta` in `ximage` we derived a 3σ upper limit of 4.2×10^{-3} s $^{-1}$ (0.3-10 keV) at the LBV star position. Using the appropriate calibration files for the date of this observation, this count rate translates into an upper limit on the unabsorbed flux of $\sim 5 \times 10^{-13}$ erg cm $^{-2}$ s $^{-1}$ (0.5-10 keV), assuming a power law model with a photon index of 2 and an absorbing column density $N_{\text{H}}=10^{22}$ cm $^{-2}$.

2.2 ART-XC

In the 4-12 keV energy range, no new sources in the *INTEGRAL* error region were reported in the first year All-sky ART-XC catalog ([Pavlinisky et al. 2022](#)) performed in 2019-2020 by Mikhail Pavlinisky ART-XC telescope onboard the Spectrum-Roentgen-Gamma mission ([Pavlinisky et al. 2021](#)). In 2022-2023, the Norma Arm region have been visited for a total time of about two ks during the new Galactic plane ART-XC X-ray survey. The upper limit 4-12 keV from possible X-ray sources in the *INTEGRAL* error radius is $F_{4-12 \text{ keV}} < 4 \times 10^{-13}$ erg cm $^{-2}$ s $^{-1}$ (90% c.l.) assuming a Crab-like spectrum. This upper limit yields an X-ray luminosity limit of $L_{4-12 \text{ keV}} < 5 \times 10^{33} (d_{10 \text{ kpc}}^2)$ erg s $^{-1}$, an order of magnitude looser than the *Chandra* limit (see below) but taken at different times than our *Chandra* observations.

3 RESULTS

In the following we report on the *Chandra* results, while the archival *Swift* observation and ART-XC limits are not discussed further.

3.1 Source detection

We performed a source detection by means of the `wavdetect` algorithm in CIAO, which uses “Mexican hat” wavelet functions with scales of 1, 2, 4, 6, 8, 12, 16, 24 and 32. We adopted a detection threshold equal to one over the area of the image in pixels, translating into approximately one spurious source (e.g., [Nandra et al. 2005](#)) inside the FOV. This resulted into 21 sources detected in the broad energy band 0.5-7 keV (Fig. 1; Table 1). Eight sources are located within the IGRJ16327 error circle, but none of them is consistent with the sky position of the LBV star (Fig. 1, right panel). We note that, if we perform a source detection with `wavdetect` in the energy bands 0.5-1.2 keV (soft), 1.2-2.0 keV (medium) and 2.0-7.0 keV (hard), usually assumed in the *Chandra* Source Catalog ([Evans et al. 2010](#)), none is detected in the soft band and most of them are detected in the hard band only.

We explored the possibility to correct the absolute astrometry using the tools `wcs_match` and `wcs_update`. They compute the fine astrometric translation shift between the list of *Chandra* detections and source lists at longer wavelengths.

We have chosen the *Gaia* DR2 catalog of optical sources which can be retrieved online by means of the software SAOImage (ds9; Joye & Mandel 2003) included in CIAO. Using `wcs_match` (with a match radius of $2''$) to cross-correlate the *Chandra* detections obtained with `wavdetect`, we got six matches with the *Gaia* catalog. However, since only two of them are located within $3'$ of the aimpoint (sources n. 1 and 6), we decided to avoid making any astrometric correction. We would like to note that there are not known secure associations of X-ray sources with other catalogs, as this region of the sky has never been observed at soft X-rays by other space missions, except for the short *Swift* observation (Sect. 2.1) which did not detect any source. Therefore, we assume here an absolute positional accuracy of $0.92''$ (90% limit, ACIS-I).¹ We note that the uncertainties on the sky coordinates reported in Table 1 are the statistical ones resulting from `wavdetect`. In the same table we report also the angular distance from the centroid of the *INTEGRAL* error circle (θ_{igr}) and the unabsorbed fluxes (0.5-7 keV) calculated using the tool `srcflux` in CIAO, adopting a power law model with a photon index of 2 and an absorbing column density of 10^{22} cm^{-2} .

Since none of the detected *Chandra* sources is consistent with the position of the LBV star, we have estimated an upper limit on the ACIS-I net count rate (99% c.l.; Kraft et al. 1991) of $R < 4.6 \times 10^{-4} \text{ count s}^{-1}$ (0.5-7 keV). Assuming an absorbed power law model with a photon index $\Gamma=2$ and an absorption column density $N_{\text{H}}=10^{22} \text{ cm}^{-2}$ (appropriate for the interstellar extinction to the star), we obtain an upper limit on the flux corrected for the absorption $\text{UF}_{0.5-10 \text{ keV}} < 1.5 \times 10^{-14} \text{ erg cm}^{-2} \text{ s}^{-1}$. Assuming the LBV distance $d=12.7_{-2.7}^{+3.2} \text{ kpc}$, it translates into an upper limit on the X-ray luminosity of $L_{0.5-10 \text{ keV}} < 2.9_{-1.1}^{+1.6} \times 10^{32} \text{ erg s}^{-1}$ (99% c.l.). We note that these uncertainties are calculated adopting the maximum and minimum values of the LBV star distance.

3.2 Spectroscopy

We extracted a spectrum from the brightest X-ray source detected within the *INTEGRAL* error radius of IGRJ16327, the source n.3 in Table 1. A simple absorbed power law is already a good deconvolution of the spectrum. We report the spectral parameters in Table 2, where we have calculated the X-ray luminosity using a distance value in units of 10 kpc, for a rapid re-scaling, since the distance is unknown. In fact, this source has no optical/NIR counterparts (see Sect. 4.2). The spectrum is shown in Fig. 2.

We extracted the spectrum also from other *Chandra* sources for which a meaningful spectroscopy can be performed. We report in Table 3 the results.

3.3 Temporal analysis

We examined the light curve (0.5–7 keV) of source n.3 trying several statistical tests on binned and unbinned data, but we did not find evidence for flaring activity or any significant variability in general (e.g., χ -square or Kolmogorov–Smirnov probability of constancy tests never resulted in vari-

ability larger than 2σ). The timing analysis of the barycentered events files did not yield any significant signal as well, with 3σ limits on the pulsed fraction of $\sim 100\%$ for a sinusoidal periodic modulation between ~ 6 and 5000 s (which is not surprising, giving the very few counts). We performed the same checks on the data of source n.14, the only one with a comparable number of net photons, but again with no positive results or meaningful upper limits.

4 DISCUSSION

Here we discuss the nature of the source IGRJ16327 in light of our *Chandra* results. First of all, we did not detect any *Chandra* source at the position of the LBV star. These findings lead to two possibilities: either the LBV star is the true optical counterpart of IGRJ16327 but displays a very low X-ray luminosity state, or one of the *Chandra* sources detected inside the *INTEGRAL* error circle is the correct association. We will discuss these two cases in Sect. 4.1 and Sect. 4.2, respectively.

4.1 Is the LBV star still a viable optical counterpart?

LBV stars are known to be at the transitional stage of evolution of very massive OB stars toward Wolf-Rayet (WR) stars characterized by a huge mass loss of about $10^{-4} M_{\odot}$ per year (Humphreys & Davidson 1994). X-ray emission from stellar winds were detected by *Chandra* and *XMM-Newton* from only a few single LBV stars (Nazé et al. 2012). The *Chandra* upper limit from WN44 obtained above is consistent with those for other LBVs. Therefore, the association of WN44 as a single LBV with the *INTEGRAL* source cannot be reliably established.

In principle, X-ray emission from an LBV can be due to accretion of stellar wind onto the secondary compact component in a binary system. From evolutionary considerations, the secondary component in this case must be the remnant of a more massive primary component, i.e. most likely a black hole.

If the hard *INTEGRAL* flare from IGRJ16327 were associated with the WN44, the maximum hard X-ray luminosity would be $L_{20-40 \text{ keV}} \approx 2 \times 10^{35} (d_{10 \text{ kpc}}^2) \text{ erg s}^{-1}$. While not excluded in principle, such flares have not been detected from other single LBVs. If the flare were due to non-stationary accretion onto the possible compact binary counterpart, the peak X-ray luminosity would correspond to a maximum accretion rate of $\dot{M}_a^{\text{peak}} \sim 2 \times 10^{15} \eta_{0.1} [\text{g s}^{-1}] \sim (3 \times 10^{-11}) \eta_{0.1}^{-1} [M_{\odot} \text{ yr}^{-1}]$ assuming the standard 10% accretion luminosity $L = \eta_{0.1} \dot{M} c^2$. This is much smaller than the expected Eddington-limited mass accretion rate in X-ray outbursts.

Very small upper limits on the quiescent *Chandra* X-ray luminosity from the *INTEGRAL* error circle, $L < 3 \times 10^{32} \text{ erg s}^{-1}$, suggest at least a three order of magnitude lower mass accretion rate onto a compact object than the *INTEGRAL* flare discussed above, $\dot{M}_a^{\text{asc}} \sim 2 \times 10^{12} \eta_{0.1} [\text{g s}^{-1}] \sim (3 \times 10^{-14}) \eta_{0.1}^{-1} [M_{\odot} \text{ yr}^{-1}]$. The Bondi-Hoyle-Littleton accretion rate from stellar wind from an LBV star with spherical mass-loss rate \dot{M}_{LBV} and the wind velocity v_w onto a compact object with mass M_x and Bondi radius $R_B =$

¹ <https://cxc.harvard.edu/cal/ASPECT/celmon>

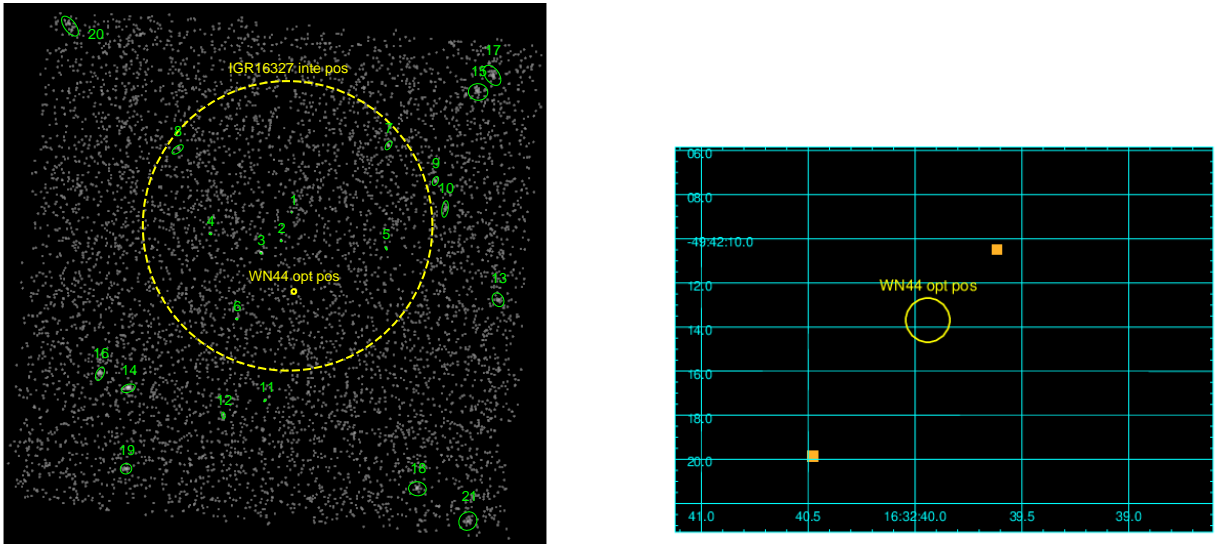


Figure 1. *Left panel:* *Chandra* ACIS-I observation (0.5-7 keV) of the IGRJ16327 field, smoothed with a Gaussian function, for presentation purposes only. The dashed yellow large circle marks the *INTEGRAL* source error circle (radius $R=5'$), while the small circle indicates the position of the LBV star (WN44). The green ellipses mark the 21 *Chandra* sources detected in the energy band 0.5-7 keV. The brightest source inside the IGRJ16327 error circle is n. 3. *Right panel:* a close-up view of the on-axis position of the ACIS-I observation is shown, together with the optical position of LBV star marked by the yellow circle ($R=1''$). Equatorial coordinates (J2000) are reported. No *Chandra* detection is consistent with the LBV star position.

Table 1. List of sources detected with *wavdetect* (0.5-7 keV). Fluxes $UF_{0.5-7 \text{ keV}}$ are corrected for the absorption and calculated with *srcflux* (uncertainties on fluxes are at 90% c.l.). θ_{igr} is the angular distance from the *INTEGRAL* centroid of IGRJ16327. “P” is the probability (%) of spurious association of the *Chandra* sources with IGRJ16327.

Source n.	R.A. (J2000) (deg)	dec (J2000) (deg)	error on R.A. (arcsec)	error on dec (arcsec)	Net counts (0.5-7 keV)	θ_{igr} (')	$UF_{0.5-7 \text{ keV}}$ ($10^{-13} \text{ erg cm}^{-2} \text{ s}^{-1}$)	P (%)
1	248.16844	-49.658329	0.18	0.15	5.80	0.48	$0.21^{+0.17}_{-0.11}$	100
2	248.17773	-49.674763	0.20	0.17	11.0	0.57	$0.51^{+0.34}_{-0.24}$	97
3	248.19571	-49.681797	0.12	0.07	46.9	1.32	1.7 ± 0.4	53
4	248.24059	-49.670654	0.41	0.19	10.7	2.68	$0.36^{+0.22}_{-0.16}$	99
5	248.08443	-49.678978	0.54	0.56	4.70	3.49	$0.18^{+0.17}_{-0.10}$	100
6	248.21715	-49.719669	0.27	0.10	17.9	3.67	$0.48^{+0.25}_{-0.19}$	97
7	248.08231	-49.619652	1.02	0.85	10.4	4.46	$0.43^{+0.27}_{-0.19}$	98
8	248.26971	-49.621994	2.01	1.09	7.10	4.62	$0.24^{+0.22}_{-0.14}$	100
9	248.04057	-49.640110	1.05	0.97	8.10	5.34	$0.32^{+0.24}_{-0.17}$	100
10	248.03203	-49.656200	1.06	1.72	8.50	5.47	$0.30^{+0.24}_{-0.16}$	100
11	248.19220	-49.766590	0.53	0.36	5.70	6.09	$0.32^{+0.27}_{-0.18}$	100
12	248.22911	-49.775108	0.64	0.81	7.00	6.91	$0.24^{+0.22}_{-0.14}$	100
13	247.98470	-49.708397	1.59	1.20	11.9	7.70	$0.48^{+0.33}_{-0.24}$	100
14	248.31387	-49.759392	0.95	0.38	54.5	7.85	2.1 ± 0.5	76
15	248.00288	-49.588818	1.98	1.11	17.4	8.04	$0.88^{+0.42}_{-0.34}$	99
16	248.33914	-49.750984	0.93	0.89	22.5	8.25	$1.00^{+0.43}_{-0.30}$	98
17	247.99036	-49.579239	1.71	1.30	20.1	8.77	$1.16^{+0.49}_{-0.39}$	98
18	248.05620	-49.817280	1.89	0.97	20.7	10.1	$0.90^{+0.40}_{-0.30}$	100
19	248.31612	-49.805748	1.28	0.75	18.6	10.1	$0.96^{+0.43}_{-0.34}$	100
20	248.36510	-49.550873	1.96	1.50	24.8	10.2	$1.22^{+0.56}_{-0.44}$	99
21	248.01111	-49.835835	1.91	1.26	18.4	11.9	$1.10^{+0.46}_{-0.40}$	100

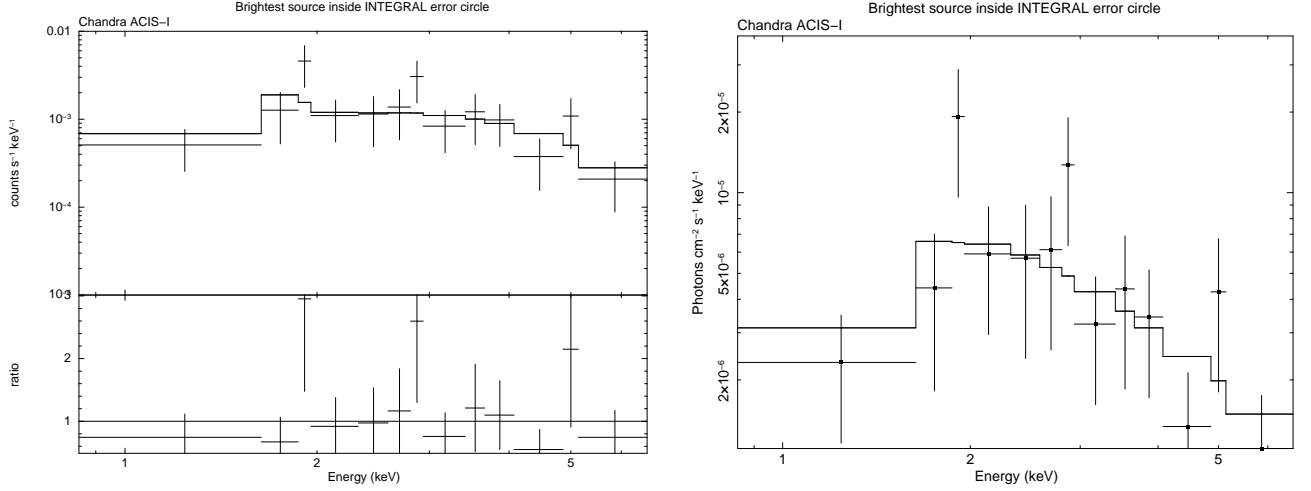


Figure 2. Spectrum of source n. 3, fitted with an absorbed power law model. The left panel shows the count spectrum together with the residuals. The photon spectrum is shown on the right. The spectra have been re-binned for presentation purposes only.

Table 2. Spectroscopy of the brightest X-ray source within the *INTEGRAL* error circle (source n. 3) adopting an absorbed power law model.

Param.	
N_{H}	$2.4^{+4.2}_{-2.3} \times 10^{22} \text{ cm}^{-2}$
Photon index Γ	$2.0^{+1.8}_{-1.3}$
$UF_{0.5-10 \text{ keV}}$	$2.5 \times 10^{-13} \text{ erg cm}^{-2} \text{ s}^{-1}$
C-Stat	35.74 (36 dof)
$L_{0.5-10 \text{ keV}}$	$3.0 \times 10^{33} d_{10 \text{ kpc}}^2 \text{ erg s}^{-1}$

$2GM_x/v_w^2$ in a circular orbit with radius a , is $\dot{M}_{\text{BHL}} \approx (1/4)\dot{M}_{\text{LBV}}(R_B/a)^2$. This is an upper limit of the actual accretion rate in the case of quasi-spherical hot radiation-inefficient accretion flows, with the reduction factor being $b = \dot{M}_a^{\text{sc}}/\dot{M}_{\text{BHL}} \sim (R_0/R_B)^{0.7}$ (Xu 2023). Assuming the compact object to be a $10 M_{\odot}$ black hole, the accretor radius is $R_0 \approx 3 \times 10^6 \text{ cm}$ and the characteristic Bondi radius is $R_B = 3 \times 10^{12} [\text{cm}] (M_x/10M_{\odot}) / (v_w/300 [\text{km s}^{-1}])^2$. Therefore, for a $10 M_{\odot}$ black hole the reduction factor in a hot accretion flow can be $b \sim 10^{-4.2}$. Thus, for the standard 10% radiation efficiency the bolometric accretion luminosity $L_{\text{bol}} = \eta_{0.1} b \dot{M}_{\text{BHL}} c^2$.

Taking the *Chandra* upper limits to the accretion luminosity, this would suggest a Bondi radius to orbital separation ratio of $(R_B/a)^2 > 10^{-8} / (b\eta_{0.1}\dot{M}_{-5})$ for the fiducial $\dot{M}_{\text{LBV}} = \dot{M}_{-5} 10^{-5} [M_{\odot} \text{ yr}^{-1}]$. Therefore, the possible orbital separation in such a binary should be $a > 10^4 R_B (b\eta_{0.1}\dot{M}_{-5})^{1/2} \sim 100 R_B$. Unfortunately, the scarcity of information about the source does not allow us to further constrain the possible binary parameters. Nevertheless, even in the case of inefficient hot accretion in a binary with a black hole component, which cannot be excluded by our *Chandra* and ART-XC X-ray limits, the appearance of a sub-luminous outburst detected by

INTEGRAL seems unnatural for non-stationary accretion as in X-ray novae.

4.2 Alternative counterparts

The lack of detection of soft X-rays at the position of the LBV star suggests alternative possibilities to uncover the nature of the *INTEGRAL* source. The best candidate soft X-ray counterpart of IGRJ16327 is the brightest *Chandra* source detected within the *INTEGRAL* error circle: the source n. 3 in Table 1. We calculated the probability of association by chance between this source and the *INTEGRAL* source as in the following. In fact, assuming the number-flux distribution ($\log N$ - $\log S$) obtained for sources in the Norma Arm region, including the AGNs (Fornasini et al. 2014; Tomsick et al. 2020):

$$N(> UF_{2-10 \text{ keV}}) = 36 (UF_{2-10 \text{ keV}} / 10^{-13})^{-1.24} \text{ deg}^{-2} \quad (1)$$

where $UF_{2-10 \text{ keV}}$ is the flux in the energy range 2–10 keV, corrected for the absorption, we find $N=0.55$ sources brighter than source n. 3 ($UF_{2-10 \text{ keV}}=1.3 \times 10^{-13} \text{ erg cm}^{-2} \text{ s}^{-1}$; Table 2) expected by chance within the *INTEGRAL* error circle ($5'$ radius). The probability that the *Chandra* source is a chance coincidence association is:

$$P = 1 - e^{-N(>UF_{2-10 \text{ keV}}) \pi \theta^2} \quad (2)$$

where θ is the angular distance (in units of degrees) of the *Chandra* source from the *INTEGRAL* position ($\theta=5'$ for sources within the *INTEGRAL* error circle, while $\theta=\theta_{\text{igr}}$, as listed in Table 1, for sources at larger distances). This implies a probability of $\sim 40\%$ of spurious association of *Chandra* source n. 3 with IGRJ16327. In Table 1 we list the probability of spurious association with IGRJ16327 for all *Chandra* sources ($P \sim 53\%$ for source n.3 if we adopt the flux obtained with `srcflux`). For all other sources this probability is much larger (and in excess of 99% for most of them).

Table 3. Spectroscopy of other *Chandra* sources, with net counts in excess of 20 (0.5-7 keV; Table 1), assuming an absorbed power law model.

Source n.	N_{H} (10^{22} cm $^{-2}$)	Γ	$UF_{0.5-10}$ keV (erg cm $^{-2}$ s $^{-1}$)	$L_{0.5-10}$ keV (erg s $^{-1}$)	C-Stat
14	$4.1^{+5.2}_{-4.1}$	$2.0^{+1.7}_{-1.5}$	$3.8^{+8.0}_{-2.8} \times 10^{-13}$	4.5×10^{33} d $_{10}^2$ kpc	40.84 (41 dof)
16	<1.7	$1.8^{+1.3}_{-0.6}$	$7.5^{+10.5}_{-2.5} \times 10^{-14}$	9.0×10^{32} d $_{10}^2$ kpc	21.44 (19 dof)
17	1.0 (fixed)	$0.7^{+1.0}_{-1.0}$	$1.5^{+1.1}_{-0.6} \times 10^{-13}$	1.8×10^{33} d $_{10}^2$ kpc	13.70 (22 dof)
18	1.0 (fixed)	$0.9^{+1.2}_{-1.2}$	$1.3^{+1.2}_{-0.5} \times 10^{-13}$	1.6×10^{33} d $_{10}^2$ kpc	11.11 (16 dof)
20	1.0 (fixed)	$1.9^{+1.1}_{-1.0}$	$1.2^{+0.8}_{-0.4} \times 10^{-13}$	1.4×10^{33} d $_{10}^2$ kpc	16.53 (18 dof)

Given these results, the source n.3 is the best soft X-ray counterpart of IGRJ16327, among the detected *Chandra* sources. Our spectral analysis indicates a quite hard X-ray emission, consistent with an X-ray binary in quiescence (Table 2), thus supporting the association with IGRJ16327.

For what concerns longer wavelengths, we searched all VizieR catalogues (via HEASARC and the ESO portal), resulting in no association of source n.3 with any counterpart. Searching the VVV survey data we obtained the following limiting magnitudes: Y=20.2, J=20.1, H=19.2 and Ks=19.0 (± 0.1 mag). However, a lower limit to the X-ray-to-optical (V magnitude) flux ratio ($F_{\text{X}}/F_{\text{opt}}$) can help in constraining its nature. We estimate this ratio adopting the limiting magnitude of the USNO-B catalogue (Monet et al. 2003) searched for counterparts ($V \gtrsim 21$ mag) and the observed X-ray source flux $F_{\text{X}} = 4.6 \times 10^{-14}$ erg cm $^{-2}$ s $^{-1}$ measured from the ACIS-I spectrum in the 0.3-3.5 energy band (Maccacaro et al. 1988), as follows: $\log(F_{\text{X}}/F_{\text{opt}}) = \log(F_{\text{X}}) + V/2.5 + 5.37$, obtaining $\log(F_{\text{X}}/F_{\text{opt}}) \gtrsim 0.433$. This value rules out a stellar coronal origin (Maccacaro et al. 1988) as well as a cataclysmic variable (Kuulkers et al. 2006) and a HMXB (Tauris & van den Heuvel 2006), leaving open the possibility of a low mass X-ray binary (LMXB) or an active galactic nucleus (AGN; Maccacaro et al. 1988).

If we assume that this *Chandra* source is the true soft X-ray counterpart of IGRJ16327, it shows an amplitude of variability of about a factor of 270 between the *INTEGRAL* luminosity re-scaled to the 0.5-10 keV energy band ($L_{0.5-10}$ keV $\sim 8 \times 10^{35}$ d $_{10}^2$ kpc erg s $^{-1}$) and the *Chandra* value (3×10^{33} d $_{10}^2$ kpc erg s $^{-1}$; Table 2), assuming the same Crab-like power law spectrum. The low X-ray luminosity in outburst and the observed dynamic range is reminiscent of the so-called very faint X-ray transients (VFXTs; Wijnands 2006; Degenaar & Wijnands 2010; Wijnands et al. 2015). This is a sub-class of LMXBs showing low outburst luminosities ($L_{\text{X}} = 10^{34}$ - 10^{36} erg s $^{-1}$) and quiescent X-ray emission at a level of $L_{\text{X}} = 10^{30}$ - 10^{33} erg s $^{-1}$. Some VFXTs certainly harbour a neutron star, given the detection of type I bursts (e.g., XMMU J174716.1-281048, Del Santo et al. 2007). The duration of their outbursts can be very variable among the members of this class, from several days to a few years. The mechanism at work producing their under-luminous X-ray outbursts is still under debate.

About the possibility of an AGN origin, the absorbing column density measured from the *Chandra* spectrum is consistent with the total Galactic value towards the source. Therefore, the intrinsic absorption of a putative AGN must be low,

indicative of either an un-observed (type 1) AGN or an intermediate type 2 Seyfert (1.8-1.9; e.g. Salvati & Maiolino 2000; Alexander 2016). Although the power law photon index of the *Chandra* spectrum is consistent with an AGN origin, the amplitude of the long-term X-ray flux variability is more difficult to reconcile with this possibility. X-ray outbursts with a similar dynamic range have been observed in the so-called quasi-periodic erupting AGN sources, possibly produced by the tidal disruption of a stellar-mass object by the central supermassive black hole (Miniutti et al. 2019). However, all the known sources displayed ultra-soft X-ray emission.

The lack of any counterpart at longer wavelengths prevents us from reaching a conclusive answer. However, while it is true that *INTEGRAL* observations have disclosed many AGNs through the Galactic plane (e.g. Malizia et al. 2020) we note that the low Galactic latitude ($b = -1.16^\circ$) favours a Galactic object.

5 CONCLUSIONS

IGRJ16327 was suggested to be a candidate HMXB hosting an LBV donor star. We proposed and performed a *Chandra* observation of the source sky position to test this hypothesis, leading to no X-ray detection at the LBV sky position. The measured upper limit to its X-ray flux of $UF_{0.5-10\text{keV}} < 1.5 \times 10^{-14}$ erg cm $^{-2}$ s $^{-1}$ (99% confidence level) allowed us to rule out the association of the *INTEGRAL* source with the LBV star.

Eight faint *Chandra* sources were detected inside the *INTEGRAL* error circle. Among them, we propose that the brightest one is the most likely soft X-ray counterpart of IGRJ16327. It displays a hard X-ray spectrum, consistent with an X-ray binary in quiescence, and no optical or NIR associations. Its X-ray luminosity is 3.0×10^{33} d $_{10}^2$ kpc erg s $^{-1}$. If this is the true counterpart of IGRJ16327, it implies a flux dynamic range of a factor of at least 270, compared with the X-ray emission of the *INTEGRAL* source extrapolated to the 0.5-10 keV energy range, adopting a Crab-like spectrum. These properties constrain the nature of IGRJ16327 either as an AGN or, more likely - given the X-ray flux variability and the location on the Galactic plane - an LMXB. In particular, we propose the identification of IGRJ16327 with a new member of the class of the VFXTs.

In any case, whatever the true counterpart, thanks to the *Chandra* observation we have obtained a clear evidence of the transient (or highly variable) nature of the source IGRJ16327.

ACKNOWLEDGEMENTS

This work is based on observations performed with the *Chandra* satellite. We made use of the software provided by the *Chandra* X-ray Center (CXC) in the application package CIAO, including SAOImage. We made use of the High Energy Astrophysics Science Archive Research Center (HEASARC), a service of the Astrophysics Science Division at NASA/GSFC. This research has made use of the VizieR catalogue service, by means of HEASARC, CDS and ESO portal. This work has made use of data from the European Space Agency (ESA) mission Gaia (<https://www.cosmos.esa.int/gaia>), processed by the Gaia Data Processing and Analysis Consortium (DPAC, <https://www.cosmos.esa.int/web/gaia/dpac/consortium>). Funding for the DPAC has been provided by national institutions, in particular the institutions participating in the Gaia Multilateral Agreement. LS thanks Manuela Molina for interesting discussions. The authors thank the anonymous referee for the very constructive report.

DATA AVAILABILITY

The *Chandra* data analysed here (ObsID 26517) are publicly available by means of the CXC or the HEASARC.

REFERENCES

- Alexander D. M., 2016, in *Active Galactic Nuclei: What's in a Name?*. p. 67, [doi:10.5281/zenodo.60525](https://doi.org/10.5281/zenodo.60525)
- Arnaud K. A., 1996, in *Jacoby G. H., Barnes J., eds, Astronomical Society of the Pacific Conference Series Vol. 101, Astronomical Data Analysis Software and Systems V*. p. 17
- Bailer-Jones C. A. L., Rybizki J., Foesneau M., Mantelet G., Andrae R., 2018, *AJ*, **156**, 58
- Bailer-Jones C. A. L., Rybizki J., Foesneau M., Demleitner M., Andrae R., 2021, *AJ*, **161**, 147
- Bird A. J., et al., 2010, *ApJS*, **186**, 1
- Bird A. J., et al., 2016, *ApJS*, **223**, 15
- Cash W., 1979, *ApJ*, **228**, 939
- Degenaar N., Wijnands R., 2010, *A&A*, **524**, A69
- Del Santo M., Sidoli L., Mereghetti S., Bazzano A., Tarana A., Ubertini P., 2007, *A&A*, **468**, L17
- Evans I. N., et al., 2010, *ApJS*, **189**, 37
- Fornasini F. M., et al., 2014, *ApJ*, **796**, 105
- Gvaramadze V. V., 2018, *Research Notes of the American Astronomical Society*, **2**, 214
- Gvaramadze V. V., 2019, *IAU Symposium*, **346**, 67
- Gvaramadze V. V., Kniazev A. Y., Fabrika S., 2010, *MNRAS*, **405**, 1047
- Gvaramadze V. V., Kniazev A. Y., Berdnikov L. N., 2015, *MNRAS*, **454**, 3710
- Humphreys R. M., Davidson K., 1994, *PASP*, **106**, 1025
- Joye W. A., Mandel E., 2003, in *Payne H. E., Jędrzejewski R. I., Hook R. N., eds, Astronomical Society of the Pacific Conference Series Vol. 295, Astronomical Data Analysis Software and Systems XII*. p. 489
- Kraft R. P., Burrows D. N., Nousek J. A., 1991, *ApJ*, **374**, 344
- Kretschmar P., et al., 2019, *New Astronomy Reviews*, **86**, 101546
- Kuulkers E., Norton A., Schwobe A., Warner B., 2006, in , Vol. 39, Compact stellar X-ray sources. pp 421–460, [doi:10.48550/arXiv.astro-ph/0302351](https://doi.org/10.48550/arXiv.astro-ph/0302351)
- Maccacaro T., Gioia I. M., Wolter A., Zamorani G., Stocke J. T., 1988, *ApJ*, **326**, 680
- Malizia A., Sazonov S., Bassani L., Pian E., Beckmann V., Molina M., Mereminskiy I., Belanger G., 2020, *New Astronomy Reviews*, **90**, 101545
- Masetti N., et al., 2010, *A&A*, **519**, A96
- Miniutti G., et al., 2019, *Nature*, **573**, 381
- Monet D. G., et al., 2003, *AJ*, **125**, 984
- Nandra K., et al., 2005, *MNRAS*, **356**, 568
- Nasa High Energy Astrophysics Science Archive Research Center 2014, HEASoft: Unified Release of FTOOLS and XANADU, Astrophysics Source Code Library, record ascl:1408.004 (ascl:1408.004)
- Nazé Y., Rauw G., Hutsemékers D., 2012, *A&A*, **538**, A47
- Negueruela I., Smith D. M., Reig P., Chaty S., Torrejón J. M., 2006, in *Wilson A., ed., Proc. of the “The X-ray Universe 2005”*, 26-30 September 2005, El Escorial, Madrid, Spain. ESA SP-604, Volume 1, Noordwijk: ESA Pub. Division, ISBN 92-9092-915-4, 2006. p. 165
- Pavlinisky M., et al., 2021, *A&A*, **650**, A42
- Pavlinisky M., et al., 2022, *A&A*, **661**, A38
- Salvati M., Maiolino R., 2000, in *Plionis M., Georgantopoulos I., eds, Large Scale Structure in the X-ray Universe*. p. 277 ([arXiv:astro-ph/0001332](https://arxiv.org/abs/astro-ph/0001332)), [doi:10.48550/arXiv.astro-ph/0001332](https://doi.org/10.48550/arXiv.astro-ph/0001332)
- Sguera V., et al., 2005, *A&A*, **444**, 221
- Tauris T. M., van den Heuvel E. P. J., 2006, in , Vol. 39, Compact stellar X-ray sources. pp 623–665, [doi:10.48550/arXiv.astro-ph/0303456](https://doi.org/10.48550/arXiv.astro-ph/0303456)
- Tomsick J. A., et al., 2020, *ApJ*, **889**, 53
- Verner D. A., Ferland G. J., Korista K. T., Yakovlev D. G., 1996, *ApJ*, **465**, 487
- Walter R., et al., 2003, *A&A*, **411**, L427
- Wijnands R., 2006, in *Meurs E. J. A., Fabbiano G., eds, Vol. 230, Populations of High Energy Sources in Galaxies*. pp 328–332, [doi:10.1017/S1743921306008581](https://doi.org/10.1017/S1743921306008581)
- Wijnands R., Degenaar N., Armas Padilla M., Altamirano D., Cavecchi Y., Linares M., Bahramian A., Heinke C. O., 2015, *MNRAS*, **454**, 1371
- Wilms J., Allen A., McCray R., 2000, *ApJ*, **542**, 914
- Xu W., 2023, *arXiv e-prints*, p. [arXiv:2305.09737](https://arxiv.org/abs/2305.09737)

This paper has been typeset from a $\text{\TeX}/\text{\LaTeX}$ file prepared by the author.